Shape optimization of geotextile tubes for sandy beach protection

Damien Isebe[†,*], Pascal Azerad[†], Frederic Bouchette[♭],
Benjamin Ivorra[†] and Bijan Mohammadi[†].

[†]Institut de Mathématiques et de Modélisation de Montpellier, Université Montpellier 2, 34095 Montpellier, France
[♭]Geosciences Montpellier, Université de Montpellier 2, 34095 Montpellier, France

01/02/2007

Abstract

The paper shows that shape optimization can be efficiently applied to ocean engineering. This is a barred beach protection study in which the solution is to dispose a new type of water wave attenuator device, called geotextile tube, in order to reduce the suspension of sediments. A general and realistic parameterization for the geotextile tube is presented and a refraction-diffraction model is used for the computation. A global optimization algorithm, able to pursue beyond local minima, is used for the search of the optimum properties of the geotextile tube.

Keywords. Shape optimization, global recursive multi-layer optimization, boundary-value problem, water wave propagation, scattering, coastal engineering.

1 Introduction

Many minimization algorithms which perform the minimization of a cost function J can be seen as discretizations of continuous first or second order dynamical systems with associated initial conditions [15]. We will see that if one introduces an extra information on the infimum, solving global optimization problems using these algorithms is equivalent to solving Boundary Value Problems (BVP) for the same equations. A motivating idea is therefore to apply algorithms solving BVPs to perform this global optimization.

In this paper we present a reformulation of global minimization problems in terms of over-determined BVPs, discuss the existence of their solutions and present an algorithm solving those problems.

The use of global optimization algorithms for shape optimization study is very important. Indeed, because of excessive cost of global optimization, techniques usually only local minimization algorithms are used for shape optimization of distributed systems, especially with fluids [12, 7]. The semi-deterministic algorithm presented here allows global optimization of systems governed by PDEs at reasonable cost.

To our knowledge, despite the fact that beach protection becomes a major problem, shape optimization techniques have never been used in coastal engineering. Groins, breakwaters or

*Email: isebe@math.univ-montp2.fr

many other structures are used to decimate water waves or to control sediment flows but their shapes are usually determined using simple hydrodynamical assumptions, structural strength laws and empirical considerations. In this study, we expose a general modelling for a new type of defense structures, namely geotextile tubes, and apply a semi-deterministic algorithm to the problem of beach protection between Sète and Marseillan (NW Mediterranean sea, Gulf of Lion, France).

In section 2, we recall the state of art on geotextiles tubes. Section 3 presents the global optimization method and mathematical background. In Section 4, the geotube modelling, the physical optimization problem are presented. Finally, Section 5 exposes and discusses optimization results.

2 Geotextile tubes

In order to decimate the water waves impact along the coastline, many devices are tested before. Until recently, the most used are emerged break-waters or groins, built by using rocks or concrete. However, these techniques require a hight cost and are not adapted, to long-term, for the beach protection because they shift the erosion process at other places instead of reducing it.

Currently, a new type of attenuator devices for the water waves acts on the coastal hydro-sedimentary system more efficiently and softly than traditional emerged brake-waters. These devices are geotextile tubes, also called geotubes (See Figure 1-**Up**). To some extent, attenuator devices in geotextile only act on the intensity of the most destroying water waves. Thus, geotubes must be, on one hand, developed on deep enough sea bottom to be sufficiently transparent w.r.t the small water waves and on the other hand, developed sufficiently far from the coastline so as to act before the water wave does not accentuate the erosive process. Practically, efficient geotextile tubes will have to make it possible to attenuate the water waves higher than 2m (called destructive water waves) and to be as transparent as possible w.r.t the water waves lower than 2m (called constructive water waves) .

This paper discusses specific shape optimization for the geotubes which solve the erosion problem in a beach protection project referring to the coast, more precisely a barred beach, between Sète and Marseillan (NW Mediterranean sea, France) (See Figure 1-**Down**). This problem is proposed by BRL engineering (BRLi), a subsidiary of the Compagnie Nationale d'Aménagement de la Région du Bas-Rhône et du Languedoc. It is a great challenge in term of optimization because a agreement is in progress for the adjustment of the site in 2008.

3 Optimization method

We consider the following minimization problem:

$$\min_{x \in \Omega_{ad}} J(x) \tag{1}$$

where $J : \Omega_{ad} \to \mathbb{R}$ is called cost function, x is the optimization parameter and belongs to an admissible space $\Omega_{ad} \subset \mathbb{R}^N$, with $N \in \mathbb{N}$. We make the following assumptions [2]: $J \in C^2(\Omega_{ad}, \mathbb{R})$ and coercive. The infimum of J is denoted by J_m.

To solve problem (1), we introduce a new class of global minimization methods based on the solution of BVP.

Figure 1: **Up-** An emerged geotextile tube; **Down-** The barred beach between Sète and Marseillan (satellite picture).

3.1 BVP formulation of optimization problems

Many minimization algorithms which perform the minimization of J can be seen as discretizations of continuous first or second order dynamical systems with associated initial conditions [14, 2].

A numerical global optimization of J with one of those algorithms, called here *core optimization method*, is possible if the following BVP has a solution:

$$\begin{cases} \text{First or second order initial value problem} \\ \min_{t\in[0,Z]}(|J(x(t)) - J_m|) < \epsilon \end{cases} \quad (2)$$

where $x(t)$ is the solution of the considered dynamical system found at time $t \in \mathbb{R}$, Z is a given finite time $Z \in \mathbb{R}$ and ϵ is the approximation precision. In practice, when J_m is unknown, we set J_m to a lower value (for example $J_m = 0$ for a non-negative function J) and look for the best solution for a given complexity and computational effort.

This BVP is over-determined as it includes more conditions than derivatives. This over-determination can be removed for instance by considering one of the initial conditions in the considered dynamical system as a new variable denoted by v. Then we could use what is known on BVP theory, for example a shooting method [14], in order to determine a suitable v solving (2).

3.2 General method for the resolution of BVP (2)

In order to solve previous BVP (2), we consider the following general method:

We introduce a function $h : \Omega_{ad} \to \mathbb{R}$ given by:

$$h(v) = \min_{t\in[0,Z]}(J(x(t,v)) - J_m) \quad (3)$$

where $x(t,v)$ is the solution of the dynamical system (2) starting from the initial condition v, defined previously, at time t. $Z \in \mathbb{R}$.

Solving BVP (2) can be performed by minimizing in Ω_{ad} function (3).

Depending on the selected optimization method, h is usually a discontinuous plateau function:

For example, if a Steepest Descent method is used as core optimization method, the associated dynamical system reaches, in theory, the same local minimum when it starts from any points included in a same attraction basin. In other words, if Z is large enough, $h(v)$ is piecewise constant with values corresponding to the local minima of $J(x(Z,v))$. Furthermore, $h(v)$ is discontinuous where the functional reaches a local maximum, or has a plateau (see Figure (2)).

Thus, one way to minimize such a kind of function is for instance to use a GA. But this method is numerically expensive. We propose a cheaper multi-layers algorithm based on line search methods [14]:

We first consider the following algorithm $A_1(v_1, v_2)$:

- $(v_1, v_2) \in \Omega_{ad} \times \Omega_{ad}$ *given*
- *Find* $v \in argmin_{w\in\mathcal{O}(v_2)} h(w)$ *where* $\mathcal{O}(v_2) = \{v_1 + t(v_2 - v_1), t \in \mathbb{R}\} \cap \Omega_{ad}$ *using a line search method*

- *return* v

The line search minimization in A_1 is defined by the user. It might fails. For instance, a secant method [14] degenerates on plateaus and critical points. In this case, in order to have a multidimensional search, we add an external layer to the algorithm A_1 by minimizing h' defined by:

$$h'(v') = h(A_1(v', w')) \tag{4}$$

with w' chosen randomly in Ω_{ad}.

This leads to the following two-layers algorithm $A_2(v'_1, v'_2)$:

- $(v'_1, v'_2) \in \Omega_{ad} \times \Omega_{ad}$ *given*
- *Find* $v' \in argmin_{w \in \mathcal{O}(v'_2)} h'(w)$ *where* $\mathcal{O}(v'_2) = \{v'_1 + t(v'_2 - v'_1), t \in \mathbb{R}\} \cap \Omega_{ad}$ *using a line search method*
- *return* v'

The line search minimization in A_2 is defined by the user.

N.B Here we have only described a two-layers structure. But this construction can be pursued by building recursively $h^i(v_1^i) = h^{i-1}(A_{i-1}(v_1^i, v_2^i))$*, with* $h^1(v) = h(v)$ *and* $h^2(v) = h'(v)$ *where* $i = 1, 2, 3, ...$ *denotes the external layer.*

During this work, we call this general recursive algorithm: Semi-Deterministic Algorithm (**SDA**). For each class of method used as core optimization method, we will describe more precisely the SDA implementation.

3.3 1st order dynamical system based methods

We consider optimization methods that come from the discretization of the following dynamical system [2, 13, 14]:

$$\begin{cases} M(\zeta, x(\zeta))x_\zeta(\zeta) = -d(x(\zeta)) \\ x(\zeta = 0) = x_0 \end{cases} \tag{5}$$

where ζ is a fictitious time. $x_\zeta = \frac{dx}{d\zeta}$. M is an operator, $d : \Omega_{ad} \to \mathbb{R}^N$ is a function giving a suitable direction.

For example:

- If $d = \nabla J$, the gradient of J, and $M(\zeta, x(\zeta)) = Id$, the identity operator, we recover the classical steepest descent method.
- If $d = \nabla J$ and $M(\zeta, x(\zeta)) = \nabla^2 J(x(\zeta))$ the Hessian of J, we recover the Newton method.

In this case, BVP (2) can be rewritten as:

$$\begin{cases} M(\zeta, x(\zeta))x_\zeta = -d(x(\zeta)) \\ x(0) = x_0 \\ \min_{t \in [0,Z]}(|J(x(t)) - J_m|) < \epsilon \end{cases} \tag{6}$$

This BVP is over-determined by x_0. i.e, the choice of x_0 determines if BVP (6) admits or not a solution. For instance, in the case of a steepest descent method, BVP (6) generally has

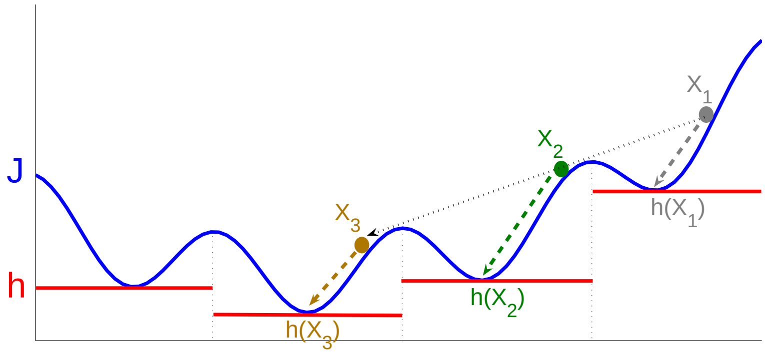

Figure 2: Graphical representation of one iteration of the algorithm A_1 considering a steepest descent method as core optimization method. $h(X_2)$ is lower than $h(X_1)$, thus X_3 is build starting from X_2 and considering the direction $\vec{X_1X_2}$.

a solution if x_0 is in the attraction basin of the global minimum. More usually, it exits a x_0 solving BVP (6): $x_0 \in argmin_{x\in\Omega_{ad}} J(x)$.

In order to determine a such x_0, we consider the implementation of algorithms A_i with $i = 1, 2, 3, ...$ (here we limit the presentation to $i = 2$).

The first layer A_1 is applied with a secant method in order to perform line search. The output is denoted by$A_1(v_1, J, I, \epsilon)$, and the algorithm reads:

Input: v_1, J, I, ϵ
v_2 chosen randomly
For l
from 1 to J
  $o_l = D(v_l, I, \epsilon)$
  $o_{l+1} = D(v_{l+1}, I, \epsilon)$
  If $J(o_l) = J(o_{l+1})$ **EndFor**
  If $min\{J(o_m), m = 1, ..., l\} < \epsilon$ **EndFor**
  $v_{l+2} = v_{l+1} - J(o_{l+1})\frac{v_{l+1}-v_l}{J(o_{l+1})-J(o_l)}$
EndFor
Output: $A_1(v_1, J, I, \epsilon)$:
    $argmin\{J(o_m), p)m = 1, ..., l\}$

where $v_1 \in \Omega$, $\epsilon \in \mathbb{R}^+$ and $(J, I) \in \mathbb{N}^2$ are respectively the initial condition, the stopping criterion and the iteration numbers. $D(v, I, \epsilon)$ is the solution returned by the core optimization algorithm starting from the initial point v after I iterations with a stopping criterion ϵ. A graphical representation of one iteration of A_1 is given by Figure 2.

The second layer A_2 is applied with a secant method in order to perform line search. The output is denoted by $A_2(w_1, K, J, I, \epsilon)$, and the algorithm reads:

Input: w_1, K, J, I, ϵ

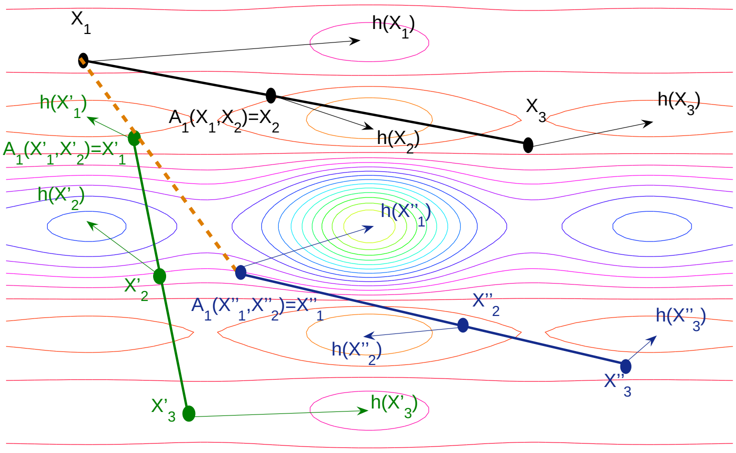

Figure 3: Graphical representation of one iteration of the algorithm A_2 considering a steepest descent method as core optimization method. Cost function $f : \mathbb{R}^2 \to \mathbb{R}$ is represented by its iso-contours.$A_1(X_1')$ is lower than $A_1(X_1)$, thus X_1'' is build starting from X_1' and considering the direction $\overrightarrow{X_1'X_1}$.

w_2 chosen randomly
For l going from 1 to K
 $p_l = A_1(w_l, J, I, \epsilon)$
 $p_{l+1} = A_1(w_{l+1}, J, I, \epsilon)$
 If $J(p_l) = J(p_{l+1})$ **EndFor**
 If $min\{J(p_m), m = 1, ..., l\} < \epsilon$ **EndFor**
 $w_{l+2} = w_{l+1} - J(p_{l+1})\frac{w_{l+1}-w_l}{J(p_{l+1})-J(p_l)}$
EndFor
Output: $A_2(w_1, K, J, I, \epsilon)$:
 $argmin\{J(p_m), m = 1, ..., l\}$

where $w_1 \in \Omega$, $\epsilon \in \mathbb{R}^+$ and $(K, J, I) \in \mathbb{N}^3$ are respectively the initial condition, the stopping criterion and the iteration numbers. A graphical representation of one iteration of A_2 is given by Figure 3.

3.4 2nd order dynamical system based methods

In order to keep an exploratory character during the optimization process, allowing us to escape from attraction basins, we could use variants of previous methods after adding second order derivatives.

For instance we could consider methods coming from the discretization of the following '*heavy ball*' dynamical system [1]:

$$\left\{\begin{array}{l} \eta x_{\zeta\zeta}(\zeta) + M(\zeta, x(\zeta))x_\zeta(\zeta) = -d(x(\zeta)), \\ x(0) = x_0, \quad x_\zeta(0) = x_{\zeta,0} \end{array}\right. \tag{7}$$

with $\eta \in \mathbb{R}$.

In this case, the associated BVP (2) is of the form:

$$\left\{\begin{array}{l} \eta x_{\zeta\zeta}(\zeta) + M(\zeta, x(\zeta))x_\zeta(\zeta) = -d(x(\zeta)), \\ x(0) = x_0, \quad x_\zeta(0) = x_{\zeta,0} \\ \min_{t\in[0,Z]}(|J(x(t)) - J_m|) < \epsilon \end{array}\right. \tag{8}$$

System (8) can be solved by considering x_0 (as previously) or $x_{\zeta,0}$ as a new variable. In the first case the existence of solution for BVP (8) is trivial. In the second case, considering particular hypothesis interesting in numerical analysis, when x_0 is fixed it can be proved that it exists a $x_{\zeta,0}$ such that BVP (8) admits numerical solutions.

3.4.1 Existence of solution for BVP (8)

The following theorem proves, considering particular hypothesis, the existence of an initial condition $x_{\zeta,0}$ solving numerically BVP (8).

Theorem 1 *Let $J : \mathbb{R}^n \to \mathbb{R}$ be a C^2-function such that $\min_{\mathbb{R}^n} J$ exists and is reached at $x_m \in \mathbb{R}^n$. Then for every $(x_0, \delta) \in \mathbb{R}^n \times \mathbb{R}^+$, exists $(\sigma, t) \in \mathbb{R}^n \times \mathbb{R}^+$ such that the solution of the following dynamical system:*

$$\left\{\begin{array}{l} \eta x_{\zeta\zeta}(\zeta) + x_\zeta(\zeta) = -\nabla J(x(\zeta)) \\ x(0) = x_0 \\ x_\zeta(0) = \sigma \end{array}\right. \tag{9}$$

with $\eta \in \mathbb{R}$, passes at time $\zeta = t$ into the ball $B_\delta(x_m)$.

Proof :

We assume $x_0 \neq x_m$. Let $\epsilon > 0$, we consider the dynamical system:

$$\left\{\begin{array}{l} \eta y_{\tau\tau}(\tau) + \epsilon y_\tau(\tau) = -\epsilon^2 \nabla J(x(\tau)) \\ y(0) = x_0 \\ y_\tau(0) = \varrho(x_m - x_0) \end{array}\right. \tag{10}$$

with ϱ in $\mathbb{R}^+\backslash\{0\}$.

- Assume that $\epsilon = 0$, we obtain the following system :

$$\left\{\begin{array}{l} \eta y_{\tau\tau,0}(\tau) = 0 \\ y_0(0) = x_0 \\ y_{\tau,0}(0) = \varrho(x_m - x_0) \end{array}\right. \tag{11}$$

  System (11) describes a straight line of origin x_0 and passing at time θ_ϱ by the point x_m, i.e. $y_0(\theta_\varrho) = x_m$.

- Assume that $\epsilon \neq 0$. System (10) could be rewritten as:

$$\left\{ \begin{array}{l} \left(\begin{array}{c} y(\tau) \\ \eta y_\tau(\tau) \end{array} \right)_\tau = \left(\begin{array}{l} y_\tau(\tau) \\ -\epsilon y_\tau(\tau) - \epsilon^2 \nabla J(y(\tau)) \end{array} \right) \\ y(0) = x_0 \\ y_\tau(0) = \varrho(x_m - x_0) \end{array} \right. \tag{12}$$

  System (12) is of the form $y_\tau = f(\tau, y, \epsilon)$, with f satisfying the Cauchy-Lipschitz conditions. Applying the Cauchy-Lipschitz Theorem [5]:
  $|y_\epsilon(\theta_\varrho) - y_0(\theta_\varrho)| \rightarrow_{\epsilon \rightarrow 0} 0$ uniformly.

  Thus for every $\delta \in \mathbb{R}^+ \backslash \{0\}$, there exists ϵ_δ such that for every $\epsilon < \epsilon_\delta$:
  $|y_\epsilon(\theta_\varrho) - x_m| < \delta$ (T.1)

Let $\delta \in \mathbb{R}^+ \backslash \{0\}$. We consider the following variable changing $\zeta = \epsilon_\delta \tau$ and $x(\zeta) = y_{\epsilon_\delta}(\frac{\zeta}{\epsilon_\delta})$. System (10) becomes:

$$\left\{ \begin{array}{l} \eta x_{\zeta\zeta}(\zeta) + x_\zeta(\zeta) = -\nabla J(x(\zeta)) \\ x(0) = x_0 \\ \dot{x}(0) = \frac{\varrho}{\epsilon_\delta}(x_m - x_0) \end{array} \right. \tag{13}$$

Let $\vartheta = \epsilon_\delta \theta_\varrho$. Under this assumption, $x(\vartheta) = y_{\epsilon_\delta}(\theta_\varrho)$. Thus, due to (T.1) : $|x(\vartheta) - x_m| < \delta$. We have found $\sigma = \frac{\varrho}{\epsilon_\delta}(x_m - x_0) \in \mathbb{R}^n$ and $t = \vartheta \in \mathbb{R}^+$ such that the solution of system (9) passes at time t into the ball $B_\delta(x_m)$.

□

3.4.2 Algorithmic implementation

In order to determine a suitable x_0 or $x_{\zeta,0}$ solving BVP (8), we can consider, for instance, the same algorithms A_1 and A_2 introduced in section 3.3.

3.5 Other hybridizations with SDA

In practice, any user-defined, black-box or commercial minimization package starting from an initial condition can be used to build the core optimization sequences in the SDA presented in section 3.2. In that sense, the algorithm permits the user to exploit his knowledge on his optimization problem and to improve it. In the same way, preconditioning can be introduced at any layer, and in particular at the lowest one.

3.6 Comparison of 1^{st} and 2^{nd} order system approaches on a benchmark function

In this section we apply algorithms, included in the class of semi-deterministic methods exposed previously, to a typical benchmark optimization problem.

We consider various versions of our SDA algorithms A_i (where i equals to 1,2 or 3) presented previously. The core optimization method is selected among the following list:

MRF	SD2A-1L	SD2A-2L	SD2A-3L	HBSDA
n=10 / $\epsilon = 10^{-6}$	Fail	1000	1500	2000
n=100 / $\epsilon = 10^{-7}$	Fail	1200	2500	3000
n=1000 / $\epsilon = 10^{-8}$	Fail	1500	5000	6000

Table 1: MRF results: Iteration number needed to obtain a reduction ϵ of the initial value of the cost function. from (**top**) to (**bottom**): $n = 10$ with a reduction $\epsilon = 10^{-6}$,$n = 100$ with a reduction $\epsilon = 10^{-7}$ and $n = 1000$ with a reduction $\epsilon = 10^{-8}$.

1- Steepest Descent method: It's defined by the following algorithm with an output called $D(x_0, I, \epsilon)$, where the inputs $x_0 \in \Omega$, $\epsilon \in \mathbb{R}^+$ are respectively the initial condition and the stopping criterion:

- **Input:** x_0, I, ϵ
- $x_1 = x_0$

For n going from 1 to I

- Determine $\rho_{opt} = argmin_\rho(J(x_n - \rho\nabla J(x_n)))$ using dichotomy
- $x_{n+1} = x_n - \rho_{opt}\nabla J(x_n)$
- **If** $J(x_{n+1}) < J_m + \epsilon$ **EndFor**

EndFor

- **Output:** $D(x_0, I, \epsilon) = x_{n+1}$

where the input I, the iteration number, is set to 10.

This algorithm denoted by **SD2A** (Steespest Descent based SDA) is used with different numbers of layer. We denotes:

- **SD2A-1L** when we consider the one-layer algorithm A_1.
- **SD2A-2L** when we consider the two-layers algorithm A_2.
- **SD2A-3L** when we consider the three-layers algorithm A_3.

2- Heavy Ball dynamical system based algorithm: We discretize system (8) [2]. The initial condition x_0 and iteration number of the core algorithm $I = 10$ are fixed, $x_{\zeta,0}$ becomes the parameter of SDA method A_2.

This algorithm will be denoted by **HBSDA** (Heavy Ball method based SDA)

In order to compare previous optimization methods we consider the minimization problem of the following modified Rastringin function:

$$J(x) = \sum_{j=1}^{n}(sin(x_j)^2 - \cos(18x_j)), x \in [-2, 2]^n \tag{14}$$

with $n = 10, 100$ and 1000. The minimum of J, $J_m = 0$, is reached at the origin. A two-dimensional representation of this function is presented by Figure 4.

This is a general non-convex function with a large number of minima. As we can observe on Table 1 $SD2A - 2L$ gives the best result in term of computational effort.

According to those results and other benchmark tests present in [6], we've decided to use the algorithm $SD2A - L2$ with the following parameters $(M, N, I, \epsilon) = (5, 5, 10, 1.e^{-6})$. These values give a good compromise between computation complexity and result accuracy. In order to simplify notations, it will be denoted by **SDA**.

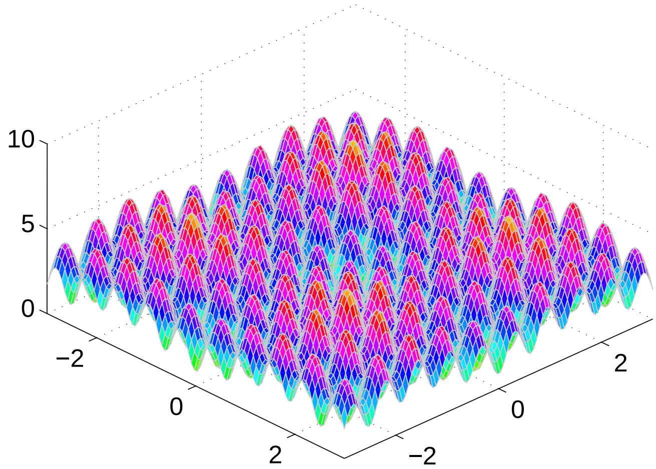

Figure 4: Modified Rastringin Function: two dimensional representation.

3.7 A particular test case

As far as we are concerned, we are particularly interested in the search of the global optimum when the control space is not connected. Actually, during the optimization of the position of geotubes, we are brought to consider a unconnected search space, due to practical, economical or political reasons which may forbid construction on a given zone. Consequently, to illustrate the efficiency of the preceding in this particular test case, we consider the minimization of an academic cost function defined on an unconnected domain. The admissible domain considered

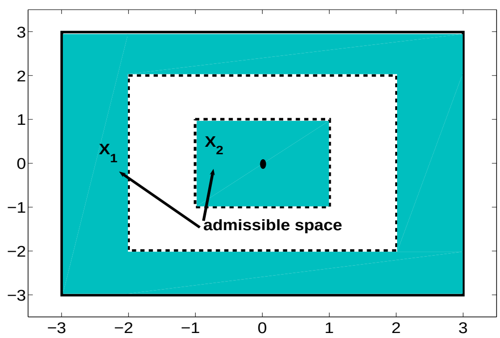

Figure 5: In grey, the admissible space Ω_{ad}

for the parameters, also called search space, is $\Omega_{ad} = X_1 \cup X_2$ with $X_1 = [-3,3] \times [-3,-2] \cup [-3,-2] \times [-2,2] \cup [2,3] \times [-2,2] \cup [-3,3] \times [2,3]$ and $X_2 = [-1,1] \times [-1,1]$ (See in Figure 5). It is clearly an unconnected domain in $\mathbb{R}^2$. The cost function to minimize is defined by

$J : X \to \mathbb{R}$ where $J(x_1, x_2) = {x_1}^2 + {x_2}^2$. It is clear that the exact global minimum of J is 0 and is obtained for $\mathbf{x}^{opt} = (x_1^{\text{opt}}, x_2^{\text{opt}}) = (0, 0)$. We choose voluntarily a starting point in X_1 because $(x_1^{\text{opt}}, x_2^{\text{opt}}) \notin X_1$. We use the steepest descent method to solve this minimization problem first in the classical form, then as a core method in our SDA. For the two optimizations, the step of descent is fixed to $\rho = 0.00001$.

For the classical gradient method, the convergence is trapped in the domain X_1 (See Figure 6-*Left*). We observe here that the algorithm cannot reach X_2 (we have chosen a small step of descent in order to be sure that the algorithm cannot reach to X_2 by luck) and what is more, it converges along the border toward the point $(-2, 0)$, a global minimum of X_1 but only a local minimum for Ω_{ad}.

Concerning the optimization using SDA, we observe that the global minimum is found. We observe, in Figure 6-*Right*, all the $\mathbf{x}^k$ tested during the optimization. The space X_2 is reached thanks to the multi-layer property of the algorithm. Indeed, the fact of considering the initial condition as a new unknown of the problem makes it possible, by the use of a shooting method, to explore the field overall. An optimal research for the step of descent is not necessary any more.

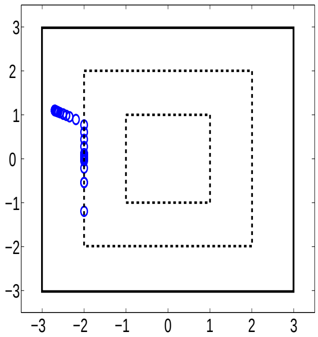

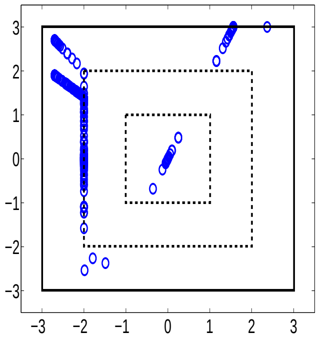

Figure 6: The circles represent all the $\mathbf{x}^k$ tested during the optimization for the computation of J. *Left*: for the classical gradient method. *Right*: for the gradient method as a core method in the SDA.

4 Geotextile tubes modelling

The Semi-Deterministic Algorithm above is used to optimize the shape of a given geotube and the distance to the coast in order to reduce the suspension of sediments that can be expressed as a function of $E = \frac{1}{8}\rho g H^2$. This energy is crucial in the erosion process. Near the coastline, the more this energy raises, the more the sediments are detached and move under the water wave action. The resulting sand loss on the beach generates erosion.

4.1 Shape design

To generalize, a geotextile tube can be compared to a large stocking made of synthetic textile and filled with sand. When it is full, the device is completely stable. Along a cross-shore profile, a general geotube can be assimilated to a flattened ellipsoid. The objective is to parameterize a geotube in our domain such that we can control its shape, position, height and width.

Before given the parameterization considered, we show, in Figure 7, the planned solution for the studied beach protection. As we can see, the improvement consists to restructure the beach and the two natural sandbars by sand recharging, and after, to place two geotubes side-by-side behind the second natural sandbar in order to protect the new beach. For the parameterization, we assume that the two geotubes side-by-side can be assimilated to one geotube twice as large.

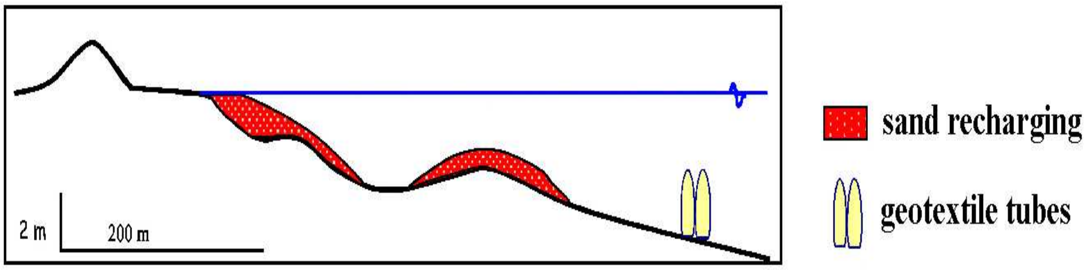

Figure 7: The improvement of the considered site

For the computation, the model uses a finite-difference mesh grid defined by a couple (mr, nr) representing the distance in the $\overrightarrow{0x}$ and $\overrightarrow{0y}$ direction. dxr and dyr are respectively the step in the x-axis and the y-axis. So, in each node (i, j), we can compute the (x, y)-coordinates by $x = (mr - i) * dxr$ and $y = (nr - j) * dyr$ and we have a value $bath(i, j)$ corresponding to the initial topobathymetry.

We parameterize the position by using a series of control points $(x_k, y_k)_{k\in\{1,\ldots,N\}}$ in the grid $[0, mr * dxr] \times [0, nr * dyr]$, where N equals the number of points used to define the geotube (two control points give a straight classical geotube instead of three or more control points give more original shape by using splines). The shape of the geotube is parameterized by the use of a gaussian function of the form $f(x) = He^{-sx^2}$ where x is the distance between a point of the mesh and its orthogonal projection on the line defining the geotube. Thus we have, in each node (i, j), a new value $addbath(i, j)$ which permit to build the new topobathymetry (see Figure 8-Left). This add two supplementaries parameters (s, H) for the control of the height and the width.

In this paper, due to industrial constraints given by BRLi, we reduce the total number of parameters to 2 by considering only the distance from the coast and the height of the geotube. We expose, in Figure 8-Right, the initial and the modified topobathymetry of the shoreface.

So, we account for the following constraints:

- The studied coastal zone is 2.4 km long.
- One geotube is considered with a length equal to the length of the beach.
- The geotube is assumed straight.
- The width is fixed to 12 m.
- The propagation is computed for water waves data at 1.2 km far from the coastline.

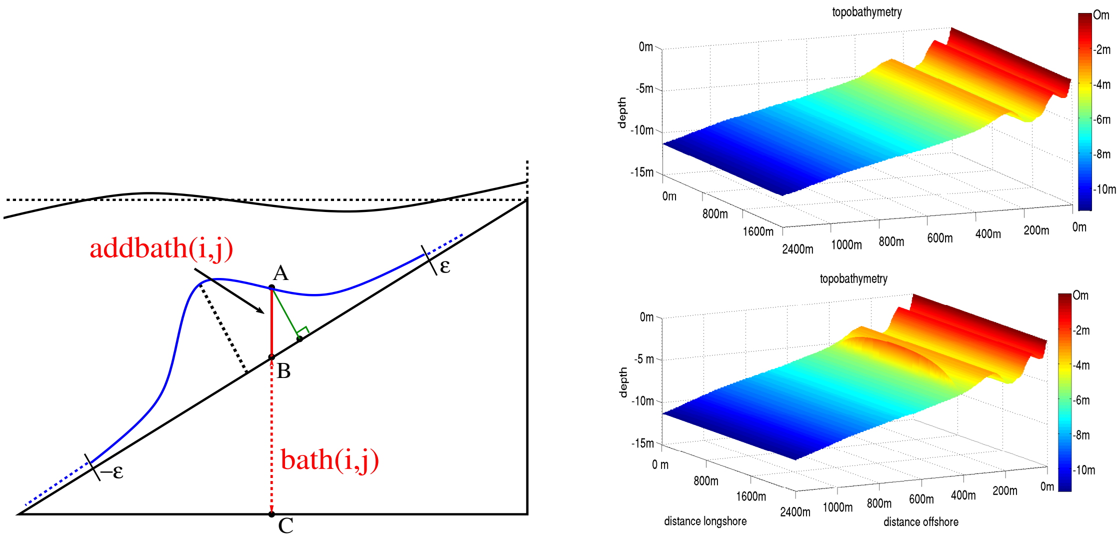

Figure 8: *Left*: The profile parameterization for the geotube in a academic linear topography; *Right*: Up- The initial topobathymetry of the barred beach, Down- Implementation of geotube in the topobathymetry. Note that both ends are smoothed by a suitable function.

- The position far from the coastline for the geotube belongs to the unconnected space $[100, 200] \cup [300, 850]$ meters, i-e the geotube cannot be located in the top of the secondly natural sandy bar.
- Starting from data given by CANDHIS (National Center Archive for In Situ Wave Data, http://www.cetmef.equipement.gouv.fr/donnees/candhis/), we compute for the two categories of the water waves (see section 2) the following mean significative height H_s, mean period T_s and mean frequency of observation p for four significant directions of propagation. We display the data in the following Table 2.

	South	South South East	East South East	East
reconstructives water waves	$H_s = 0.76$m $T_s = 4.96$s $p = 24.66\%$	$H_s = 0.85$m $T_s = 5.21$s $p = 22.75\%$	$H_s = 0.85$m $T_s = 5.21$s $p = 22.75\%$	$H_s = 0.66$m $T_s = 4.99$s $p = 17.5\%$
destructives water waves	$H_s = 2.91$m $T_s = 7.54$s $p = 2.84\%$	$H_s = 3.233$m $T_s = 7.78$s $p = 3.25\%$	$H_s = 3.233$m $T_s = 7.78$s $p = 3.25\%$	$H_s = 3.55$m $T_s = 8.03$s $p = 2.5\%$

Table 2: Hydrodynamics data for the computation

4.2 State equation

The water wave propagation and the transformation of a forward scattered wave field along an irregular mild slope is computed by using the refraction-diffraction model REF/DIF developed at the Center for Applied Coastal Research (University of Delaware, US) [8, 9]. This program is implemented in Fortran.

This finite-difference model is based on a combination between the following elliptic mild-slope equation [3, 16, 4]

$$\nabla \cdot (CC_g \nabla \xi) + \omega^2 \left(\frac{C_g}{C} \right) \xi = 0 \tag{15}$$

where h is the depth, k the wave number, g the gravity acceleration, $C = \sqrt{\frac{g}{k} \tanh kh}$ the velocity of the wave and $C_g = C \frac{(1+\frac{2kh}{\sinh 2kh})}{2}$ the group velocity, and the following parabolic model for the diffraction [11, 10],

$$2i \frac{\partial A}{\partial x} + \frac{1}{k} \frac{\partial A^2}{\partial^2 y} - K'|A|^2 A = 0 \tag{16}$$

where A the complex amplitude such that $\xi(x, y) = A(x, y)e^{ikx}$ and

$$K' = k^3 \left(\frac{C}{C_g} \right) \frac{\cosh 4kh + 8 - 2\tanh^2 kh}{8 \sinh^4 kh}. \tag{17}$$

Moreover, the wave number satisfies the dispersion equation

$$w^2 = gk \tanh kh \tag{18}$$

where ω is the angular frequency.

4.3 Cost function

The longshore sediment drift is mainly due to water waves breaking on the barred beach with a big mechanic energy.

The aim of the device is to prematurely release this energy by breaking the water waves sufficiently far away from the coastline.

Dire ici la zone choisi et pourquoi?

However, as we have seen in section 2, we consider two categories of water waves for the study, the constructive and the destructive ones, and we consider the following cost function to minimize

$$J = \frac{\int_D E_{destruc} ds}{\int_D E_{construc} ds} \tag{19}$$

where, for a point (x_i, y_i) in $D = [100, 250] \times [0, 2400]$, the energy is given by the expression

$$E(x_i, y_i) = \frac{1}{8} \rho g H(x_i, y_i)^2 \tag{20}$$

where ρ is the water density and $H(x_i, y_i) = 2A(x_i, y_i)$.

From a physical point of view, this cost function aim at decreasing the energy for the destructive water waves and to be non active for the constructive water waves.

5 Results and discussion

In order to show that global optimization is of great interest for coastal engineering, we fix the height of the geotube to 3m, sample the offshore distance between 100 and 750 seaward. We compute the cost function value for a geotube located at each sampled position. We obtain the cost function evolution w.r.t the geotube position presented in Figure 9. We clearly see that the minimum is obtained for a geotube located about 350m far from the coastline and that the

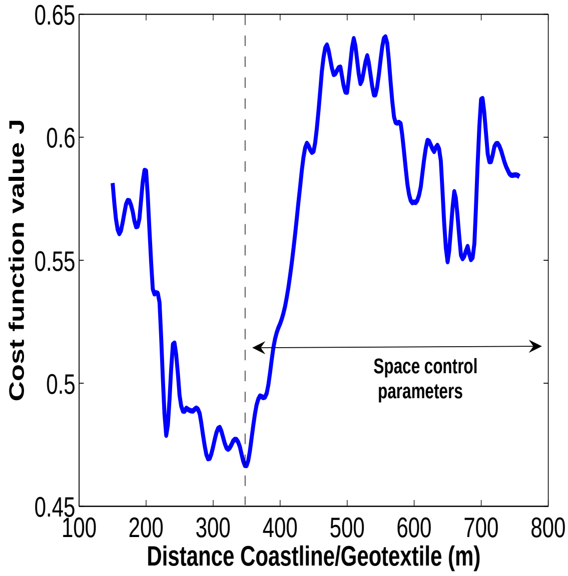

Figure 9: Cost function evolution w.r.t to the geotube position

cost function is obviously non-convex. The objective here is to recover the global optimum by starting the algorithm in a local attraction basin. The optimization problem is performed using the two-layer algorithm A_2 with a conjugate steepest descent algorithm as core optimization method. Each steepest descent iteration number equals to 100. The layer iteration number is set to 5 (i.e. $K = L = 5$). SDA starts from an initial topobathymetry created with a geotextile tube located 550m far from the coast with a height of 3m. The optimal configuration is obtained for a geotube located 353m far from the coast with a height equals to 2.5m. We can observe, in Table 3, that the optimized geotube is, on the one hand, transparent for the constructive water waves, i-e it does not affect the small water waves, and on the other hand, efficient for the four propagation directions considered, i-e it significantly weakens the energy in each case compared to the topography without geotube. In general, the cost function is reduced by 21% with this optimized geotube. We show the cost function convergence histories in Figure 10. We point out that SDA has visited several attraction basins before exploring the best element basin. Each state evaluation requires about 15 min on a 3 GHz 1 Gb Ram PC computer. To illustrate, we show in Figure 11 the comparison between the height H resulting from the propagation over the optimized geotube and the height for a water waves propagation over the initial barred beach topobathymetry. The water wave considered is a destructive water wave with a direction of propagation SSE. We notice that H is indeed lower between 100 et 250 meters far from the coast when we locate a geotube to 353 meters of the coast. This shows us that a geotube laid immediately downstream from the second natural sandy bar makes it possible to break the water wave close to the coast. Moreover, the Figure 12 ensures us that this optimized configuration does not increase the bottom orbital velocity, the fluid particle velocity, compared to the initial configuration. One is thus assured that shearing at the bottom is not amplified by this optimal configuration.

	South	South South East	East South East	East
constructive water waves	==	==	==	==
destructive water waves	15% gain	30% gain	16% gain	15% gain
global gain	21%			

Table 3: Optimization results in terms of cost function considered

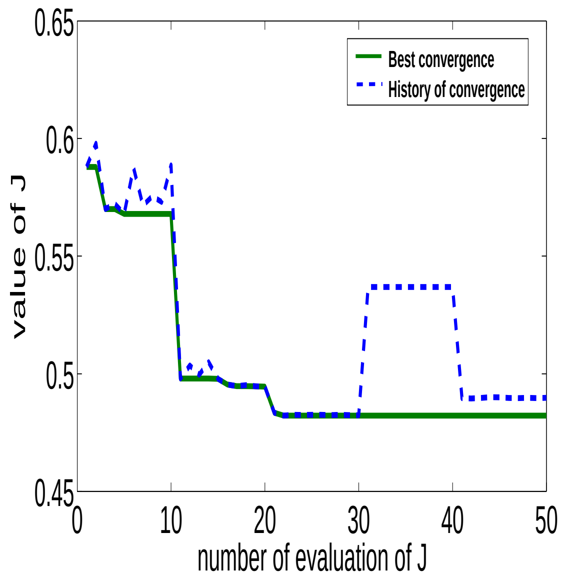

Figure 10: Cost function convergence during the optimization

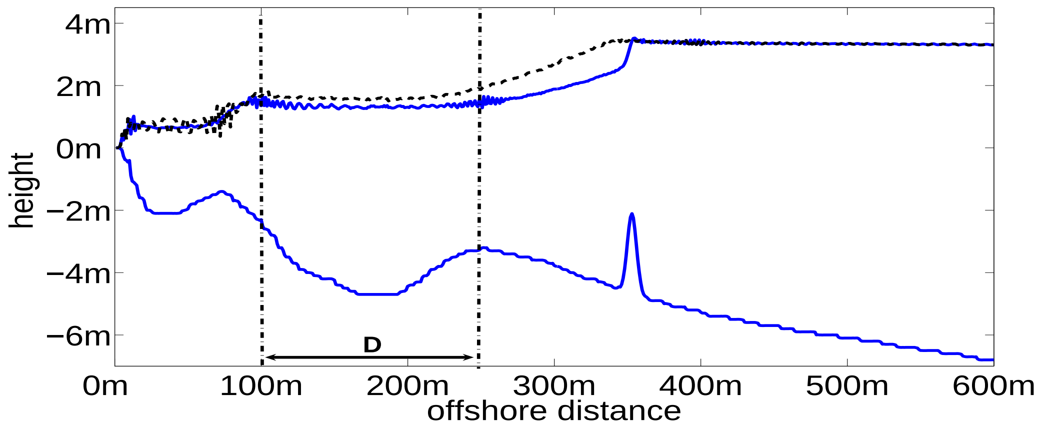

Figure 11: (solid line) Profile view of the topobathymetry including the optimized geotube and the resulting height H - (dashed line) the height H resulting of the propagation on the initial topobathymetry without geotube.

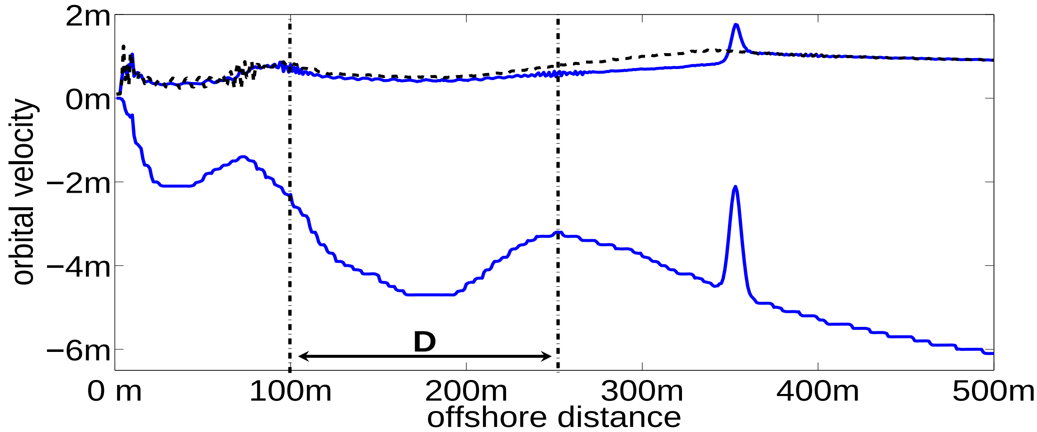

Figure 12: (solid line) Profile view of the topobathymetry including the optimized geotube and the resulting orbital velocity U_{orb} - (dashed line) the orbital velocity U_{orb} resulting of the propagation on the initial topobathymetry without geotube.

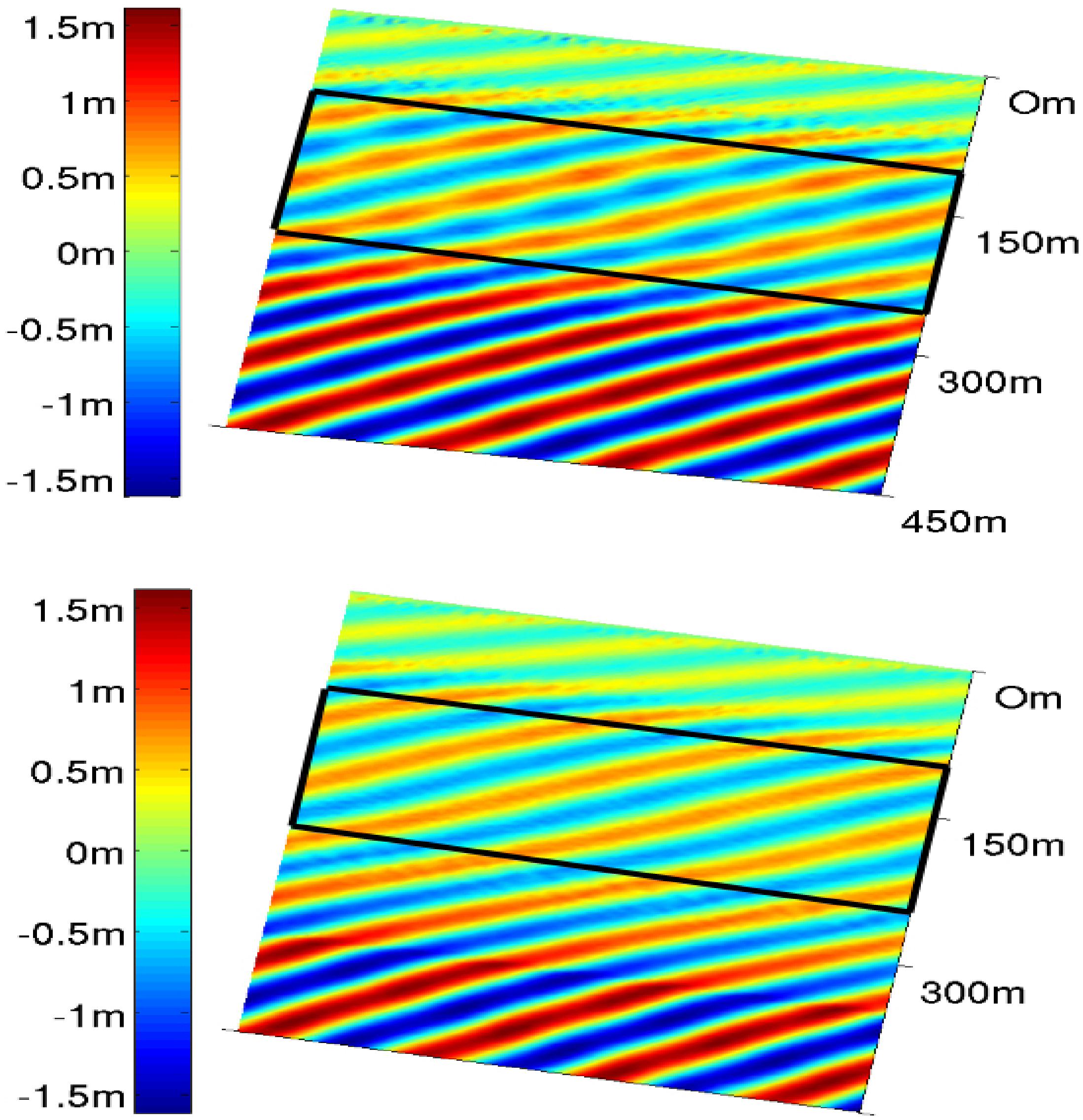

Figure 13: free surface elevation for a East destructive water wave on (Up)- the initial topobathymetry; (Down)- on the optimized topobathymetry

6 Conclusion

An specific formulation for deterministic global optimization based on the solution of initial and boundary-value problems (BVPs) for the steepest descent method has been presented. It is applied in a particular beach protection problem similar to the ones we study in coastal engineering. The obtained results are satisfactory of course they could be improve by increasing the number of control parameters to construct the geotextile tube.

7 Acknowledgements

This work is part of the COPTER research project (2006-2009) NT05 - 2-42253 funded by French National Research Agency, which we gratefully acknowledge.

References

[1] H. Attouch and F. Alvarez. The heavy ball with friction dynamical system for convex constrained minimization problems. *Lecture Notes in Economic and Mathematic Systems*, 481:25–35, 2000.

[2] H. Attouch and R. Cominetti. A dynamical approach to convex minimization coupling approximation with the steepest descent method. *Journal of Differential Equations*, 128(2):519–540, 1996.

[3] J. C. W. Berkhoff. Computation of combined refraction-diffraction. In ASCE., editor, *Proc. 13th Coastal Eng. Conf., Vancouver*, pages 471–490, 1972.

[4] N. Booij. Gravity waves on water with non-uniform depth and current. *(PhD thesis) Technical University of Delft, The Netherlands*, 1981.

[5] Verhulst F. *Nonlinear differential equations and dynamical systems.* Springer-Verlag., 1990.

[6] B. Ivorra. Semi-deterministic global optimization. *PhD. University of Montpellier 2*, 2006.

[7] A. Jameson, F. Austin, M.J. Rossi, W. Van Nostrand, and Knowles G. Static shape control for adaptive wings. *AIAA Journal*, 32(9):1895–1901, 1994.

[8] J. T. Kirby and R. A. Dalrymple. A parabolic equation for the combined refraction diffraction of stokes waves by mildly varying topography. *J. Fluid. Mechanics.*, 136:443–466, 1983.

[9] J. T. Kirby and R. A. Dalrymple. Refdif1 v2.5 refraction diffraction model. *Technical report, CACR. Short A.D 1999. Beach and Shoreface Morphodynamics.*, Wiley:380pp, 1995.

[10] C.C. Mei and E.O. Tuck. Forward scattering by long thin bodies. *SIAM J. Appl. Math.*, 39(1):178–191, 1980.

[11] C.C. Mei and D.K.P. Yue. Forward diffraction of stokes waves by a thin wedge. *J. Fluid Mech.*, 99(1):33–52, 1980.

[12] B. Mohammadi and O. Pironneau. *Applied shape optimisation for fluids.* Oxford University Press, 2001.

[13] B. Mohammadi and O. Pironneau. *Applied Shape Optimization for Fluids.* Oxford University Press, 2001.

[14] B. Mohammadi and J-H. Saiac. *Pratique de la simulation numérique*. Dunod, 2002.

[15] B. Mohammadi and J-H. Saiac. *Pratique de la simulation numérique*. Dunod, 2003.

[16] A. C. Radder. On the parabolic equation method for water-wave propagation. *Journal of Fluid Mechanics*, 95(1):159–176, 1979.